Simulation and Modeling of Physical Vapor Deposition (PVD) Process

Ali MOARREFZADEH
Faculty Member of Mechanical Engineering Department,
Mahshahr Branch,
Islamic Azad University, Mahshahr, Iran
A.moarefzadeh@mahshahriau.ac.ir

Abstract: The deposition of thin film layers from the vapor phase is accomplished through several techniques. We review the physical vapor deposition (PVD) techniques and equipment that are in common use in the high-volume production of coatings that find application in the optical, display, decorative and tribological. Specific PVD processes and coating materials have been developed and optimized for each application. It is well established that low pressure physical vapor deposition processes such as thermal evaporation and the many variants of sputtering utilize nearly collision less vapor transport to a substrate. This results in line-of-sight deposition. The deposition of uniform coatings on complex shapes using these approaches therefore requires substrate rotation or a multiple evaporation source strategy. In many cases, the line-of-sight requirement precludes the use of these processes entirely. Recently, developed rarefied gas jet based deposition processes, however, operate at much higher pressures where many gas phase collisions occur. Direct simulation Monte Carlo (DSMC) simulations have been used to understand the fundamental phenomena involved and to identify the role of the process conditions on the coating's uniformity.

Key-Words: Modeling, Simulation, workpiece, coating, Surface, PVD

1 Introduction

Physical vapor deposition (PVD) covers a broad class of vacuum coating processes in which material is physically removed from a source by evaporation or sputtering, transported through a vacuum or partial vacuum by the energy of the vapor particles, and condensed as a film on the surfaces of appropriately placed parts or substrates.

A family of very versatile coating processes in which a material is converted to its vapor phase in a vacuum chamber and condensed onto a substrate surface as a very thin film. The deposition of thin film layers from the vapor phase is accomplished through several techniques. We review the physical vapor deposition (PVD) techniques and equipment that are in common use in the high-volume production of coatings that find application in the optical, display, decorative, tribological, and energy-generating /saving industries.

Coating materials are classified as dielectric compounds, metals, alloys, or mixtures. The same material can exhibit different optical, electrical, and mechanical properties depending on the deposition process. Titanium oxide is a unique example of a metal oxide compound that, depending on deposition process parameters, can be made into film layers that are: transparent, electrically conductive, chemically reactive to light and bio-agents, chemically inert, or exhibit spectrally selectively absorption.

The dependent parameters are starting composition, oxidation state, crystalline structure and packing density.

PVD techniques used in production are basically two in nature: thermal evaporation by resistively heating or by using an electron- beam heating, and sputtering, a no thermal process. Variations and additions are made to the basic PVD techniques to per- mit different coating materials and substrate types to be accommodated. Process additions designed to alter the growth nano-structure or composition of the film through control of the dependent variables listed above include bombardment of the growing film by high energy inert- or / and reactive ions, substrate heating, atmosphere composition and partial pressure, rate, and vapor incidence angle. A further important variable contribution to the nucleation and self-assembling growth structure of the condensing ad atoms, that we have discussed frequently, is the

condition both chemical and physical of the substrate surface (PVD process shows in Figs.1,2).

• Varieties of coatings can be deposited such as metals, alloys, ceramics and other inorganic compounds, and even certain polymers.
• Deposition can be done onto the varieties of substrates such as metals, glass, and plastics.

The properties of atavistically deposited films depend strongly on:

• The material being deposited
• Substrate surface chemistry and morphology
• The surface preparation process
• The details of deposition process and the deposition Parameters.

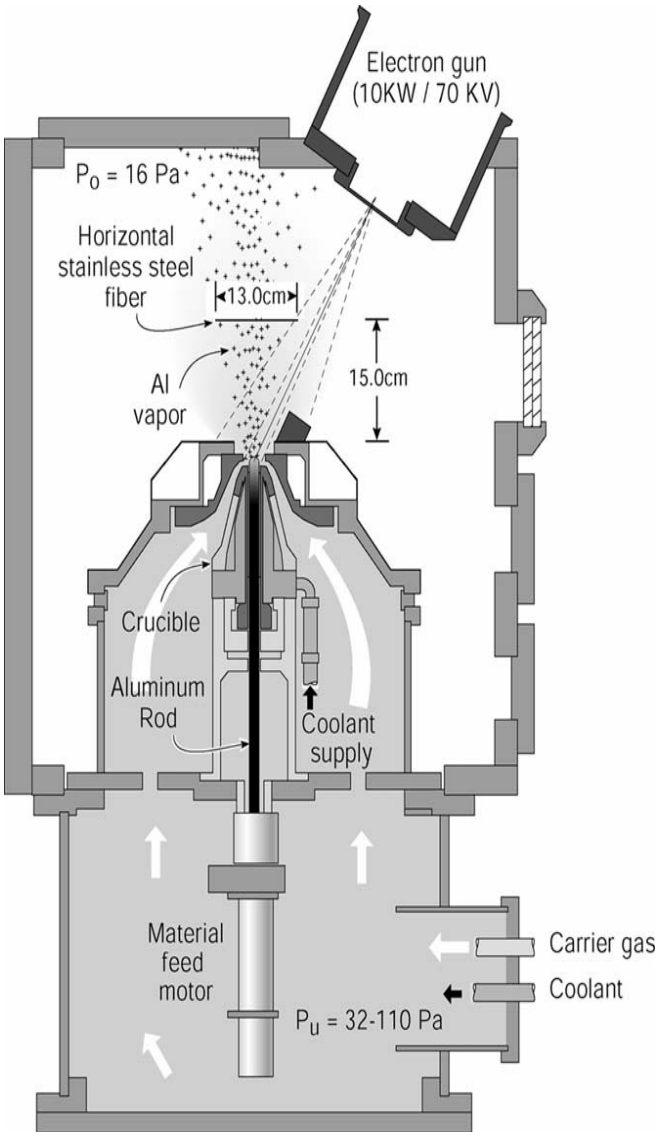

Fig. 1. Schematic illustration of a directed vapor deposition coating system[2]

Condensation and nucleation- Atoms that impinge on a surface in a vacuum environment may be reflected immediately, re-evaporate after a residence time, or condense on the surface.

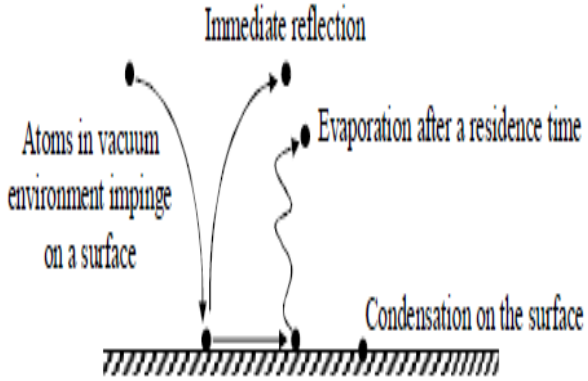

Fig.2. PVD process[1]

sticking coefficient is defined as the ratio of the condensing atoms to impinging atoms.
If the atoms do not immediately react with the surface, they will have some degree of surface mobility over the surface before they condense.
Re-evaporation is a function of bonding energy between the adatom and the surface, the surface temperature, and the flux of mobile adatoms.
Example: The deposition of cadmium on a steel surface having a temperature greater than about 200 ˚C will result in total re-evaporation of the cadmium.

2 Surface mobility

The ability of an atom on a surface will depend on the energy of the atom, atom-surface interaction (chemical bonding), and the temperature of the surface. The mobility on a surface can vary due to changes in chemistry or crystallography. The different crystallographic plates of a surface have different surface free energies that affect the surface diffusion.

Atoms condense on a surface by losing energy. They lose energy by:
-Making and breaking chemical bonds with the substrate atoms.
-Finding preferential nucleation sites
(lattice defects, atoms steps, impurities)
-Colliding with other diffusing surface atoms
(same species)
-Colliding or reacting with adsorbed surface species (Fig.3)

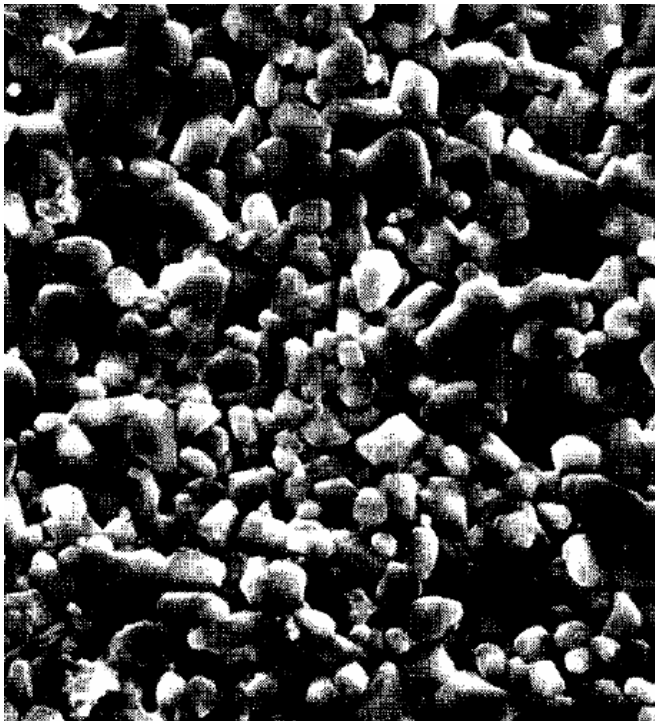

Fig.3. Surface morphology of an glass bonded (Si-O) sintered 96% alumina Ceramic

When atoms condense they form nuclei. If the surface is of the same material as the deposition atoms, the process is called homogenous nucleation and if they are different materials, the process is called heterogeneous. In semiconductor terminology, heterogeneous nucleation forms heterojunctions.
Three types of nucleation mechanisms have been identified; they differ according to nature of interaction between the posited atoms and the substrate material:

• Frank-Van der Merwe mechanism leading to a monolayer-by-monolayer growth (layer growth; ideal epitaxy)

Volmer-Weber (V-W) mechanism, characterized by a three-dimensional nucleation and growth (island growth)

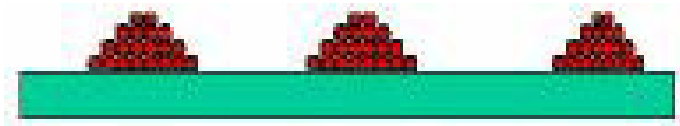

Stranski-Krastanov (S-K) mechanism, where an altered surface layer is formed by reaction with the deposited material to generate a strained or pseuomorphic structure, followed by nucleation on this layer (Layer + island growth)

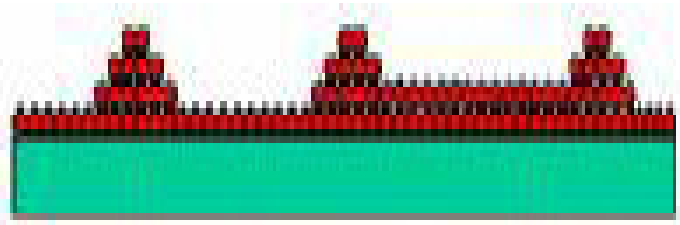

Nuclei coalescence and agglomeration The nuclei grow by collecting atoms that diffuse over the surface. Isolated nuclei grow laterally and vertically on the surface to form a continuous film. The higher the nucleation density, the less the amount of material needed to form a continuous film.

The principal growth mode of nuclei may be:
-laterally over the substrate surface (wetting growth) such as gold on copper and chromium, iron on W-O surfaces, and titanium on SiO2 the nuclei may prefer to grow in a vertical mode (dewetting growth) such as nickel and copper on W-O surfaces, and gold on carbon, Al2O3, and SiO2. Growth and coalescence of the nuclei can leave interfacial voids or structural discontinuities at the interface, particularly if there is no chemical interaction between the nuclei and substrate material and dewetting growth occurs.

3 PVD Film Evaluation

In a production environment, films are typically evaluated for visual defects, thickness, and adhesion. Visual defects such as bare spots, small voids, incorporated flakes, or debris can be observed with a stereo microscope having a magnification of 10 to 100 times.
Film thickness is generally measured by one of the following methods:
· Polished metallurgical micro sections are used to microscopically observe the coating thickness on various part surfaces. This method is the most direct way to determine thickness uniformity.
· Beta (high-energy electron) backscatter instruments are used to measure the film thickness nondestructively. This is an indirect method that requires calibration with a known standard; substantial errors can be made in measuring the film thickness on curved surfaces if care is not exercised.
· A ball-crater instrument can be used to polish through the surface of a coating.

The relationship between the diameter of the polishing ball, the maximum diameter that shows the effects of

polishing, and the diameter of the substrate area that is exposed by polishing is used to calculate the thickness. Coatings that are up to 120 m-in. (3Mm) thick can be measured with an accuracy of±4 m-in. (±0.1 Mm) without difficulty on relatively smooth, flat or cylindrical surfaces.

The adhesion between coating and substrate is difficult to measure directly for highly adherent films; pull tests capable of measuring yield strengths that are typical of metals and PVD hard coatings on metals have not been developed. A commonly used indirect test is the manual stone abrasion test (SAT).

In this test, a fine sharpening stone is rubbed back and forth across the coated surface, allowing the stone particles to make grooves in the surface by nonrealistic deformation. The film is then inspected under a microscope to obtain adhesion information.

4 Experimental observations

Scanning electron microscope (SEM) micrographs of the cross section of the fibers coated with aluminum are shown in Fig. 2 for the three pressure ratio conditions. In each case, the micrographs are taken from the midpoint of the wire and therefore correspond to the structure created on the axis of the jet. This location led to the lowest uniformity of any point on the fiber, see Table 2.

In Fig. 4, the relative coating thicknesses are plotted as a function of the position around the periphery of the fiber[11]. Note that when the pressure ratio was high (i.e. 7.0) the backside coating thickness was less than 10% of the front side. When the pressure ratio was reduced to 4.5, the backside coating thickness increased and at the lowest pressure ratio, 2.0, the backside coating thickness was greater than 70% of the front side thickness. The maximum thickness of the coatings on the front side (normalized by the amount of material evaporated in each case) was also reduced when the pressure ratio was decreased from 7.0 to 2.0, Table 1.

Table 1
Summary of the deposition time and evaporation rates used for each experiment. The frontside thickness on the fiber is given for each case, as is the thickness
normalized by the evaporation rate.

Pressure ratio	Deposition time (min)	Evaporation rate (mg/min)	Frontside thickness (μm)	Normalized frontside thickness (μm/mg/min)
7.0	3	67	87	1.29
4.5	6	58	59	1.01
2.0	12	53	31	0.58

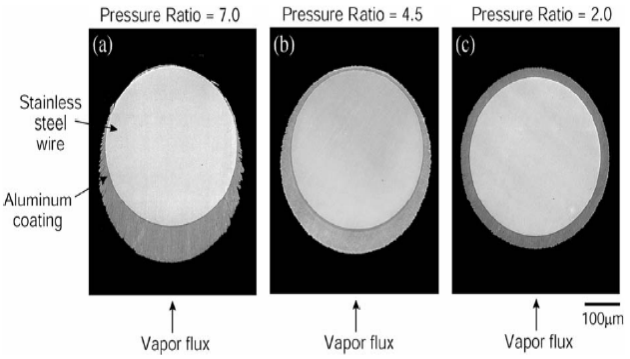

Fig.4. SEM micrographs showing cross sections of aluminum coatings deposited onto stainless steel fiber substrates (380 Am diameter) using a pressure ratio of (a) 7.0, (b) 4.5 and (c) 2.0. Note the dramatic increase in the coating thickness on the backside of the fibers as the pressure ratio was decreased.

Table 2
Ratio of the front side coating thickness to the backside coating thickness for a given distance from the jet axis

Distance from jet axis (cm)	Pressure ratio=2.0
0.0	0.72
1.0	0.73
2.0	0.75
3.0	0.76
4.0	0.77
5.0	0.88

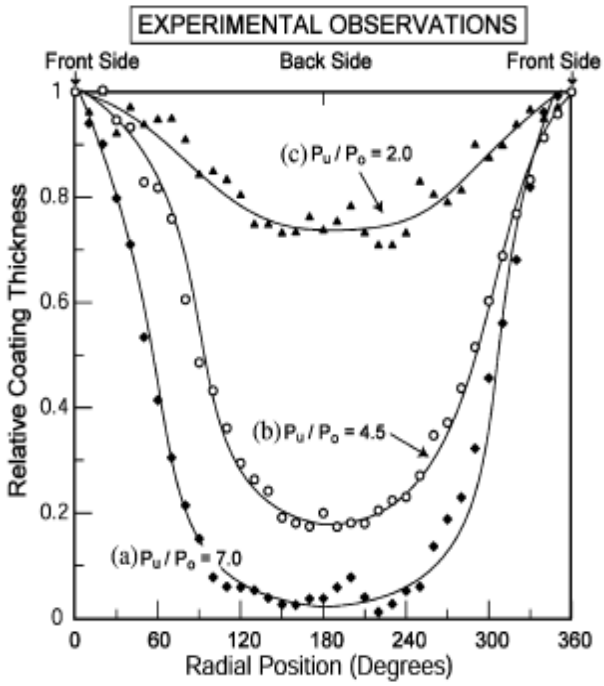

Fig. 4. Plot showing the relative coating thickness as a function of radial position on the fiber using a pressure ratio of (a) 7.0, (b) 4.5 and (c) 2.0.

5. Simulations

A DSMC code (Icarus) developed at Sandia National Laboratories was used to determine the velocity field of the gas jet for the three test conditions. It was also used to analyze the interaction between the gas jet, the vapor flux and a polygonal approximation to a cylindrical fiber. We first simulated the expansion of a helium gas jet from a choked nozzle in the absence of a cylindrical substrate. The flow field was determined at the substrate location and used in a second model to analyze the interaction of the flow with the cylindrical substrate. The inputs to the substrate interaction model were the velocity of the gas flow and the vapor flux at the position of the substrate (determined from the preceding analysis). Previous simulations have indicated that the vapor atoms reach the velocity of the gas jet a short distance from the source and thus the aluminum vapor atoms were input at the same velocity as the helium. The average trajectories of the helium and aluminum atoms and the helium velocity in the axial direction were determined for a region near the cylindrical substrate.

The use of a rarefied gas jet to alter vapor atom trajectories has allowed the coating of regions on a circular cross section that were not in the line-of-sight of the vapor source. The degree of non-line-of-sight deposition and thus the coating thickness uniformity was a sensitive function of the gas jet flow conditions. For a fixed background pressure in the region of deposition, an increase in coating uniformity was observed as the jet's Mach number was reduced.

DSMC analysis has indicated that the observed NLOS coating is a result of binary collisions between carrier gas and vapor atoms in the flow. The analysis shows that gas jet streamlines flow around the substrate. Scattering from the carrier gas streamlines allows the aluminum vapor atoms to diffuse out of the flow and impact parts of the substrate that are not directly viewable from the source.

The transport of vapor atoms in a gas jet depends on several factors: the Mach number (or kinetic energy) of the gas jet and vapor atoms, the Knudsen number of the gas jet and vapor atoms (The Knudsen number, Kn, is defined as the ratio between the mean free path in a flow to the characteristic length of a body immersed in the flow.

As the Mach number DVD gas jet varied from 0.433 to 0.039, Kn for Al–He scattering was estimated to change to 0.6 to 0.3) and the mass of the two atom types present. High gas jet Mach numbers (>0.3) and small Knudsen numbers (<0.1) promote vapor atom transport close to the gas jet atom flow trajectories since collisions between vapor and gas jet atoms occur frequently and are energetic. This results in limited vapor atom diffusion perpendicular to the streamline and, for the fiber case, leads to a low deposition flux contribution via scattering. When the Mach number is reduced and/or the Knudsen number increased (Knudsen numbers much greater than one are not desired since vapor atoms may then be carried past the fiber without scattering from the streamlines), collisions between the carrier gas and the vapor atoms occur less frequently and the momentum of the carrier gas is lowered (Knudsen numbers much greater than one are not desired since vapor atoms may then be carried past the fiber without scattering from the streamlines).

To estimate the coating thickness around the circumference of the fiber in the simulation, we computed the aluminum vapor density at a distance less than 10 Am from the surface of the cylindrical substrate. This distance was small compared to the mean free path and the fiber diameter. The results are plotted as a function of the radial position on the substrate's circumference in Fig. 5. As the Mach number was decreased, the predicted uniformity of the aluminum coating around the fiber's circumference improved. This result was similar to that seen in the experimental study, Fig. 3.

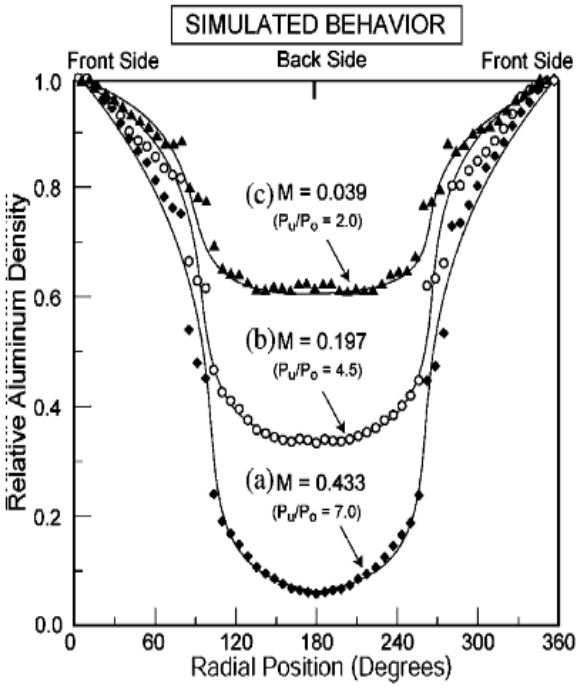

Fig.5. Plot showing the relative aluminum density above the fiber surface as a function of radial position on the fiber for a gas jet Mach number of (a) 0.433, (b) 0.197 and (c) 0.039. Note the general increase in uniformity as the Mach number was decreased compared well with the experimental observations.

6 Conclusion

Coatings of aluminum having good uniformity (backside coating thickness >70% of front side coating thickness) have been produced on stationary, non-

rotated, cylindrical substrates using a increased pressure PVD technique that incorporates the use of a gas jet. The thickness uniformity around the fibers circumference was a sensitive function of the gas jet Mach number. Low gas jet Mach numbers led to the highest uniformity since binary collisions between the gas jet and the aluminum atoms promoted diffusive transport that resulting in online- of-sight coating.

References

[1] T. Suzuki, H. Umehara, Carbon 37 (1999) 47.

[2] P.R. Subramanian, S. Krishnamurthy, S.T. Mendiratta, Mater. Sci. Eng. A 244 (1998) 1.

[3] T. Kaneko, O. Nittono, Surf. Coat. Technol. 90 (1997) 268.

[4] F. Lantelme, A. Salmi, B. Coffin, J. Claverie, Y. Le Petitcorps, Mater.Sci. Eng. B 39 (1996) 202.

[5] Z. Shi, X. Wang, Z. Ding, Appl. Surf. Sci. 140 (1999) 106.

[6] S.V. Sotirchos, S.F. Nitodas, J. Cryst. Growth 234 (2002) 569.

[7] F.S. Shieu, M.H. Shiao, Thin Solid Films 306 (1997) 124.

[8] J.H. Miller, P.K. Liaw, J.D. Landes, Mater. Sci. Eng. A 317 (2001) 49.

[9] K.A. Appiah, Z.L. Wang, W.J. Lackey, Carbon 38 (1999).

[10] T.J. Hwang, M.R. Hendrick, H. Shao, H.G. Hornis, A.T. Hunt, Mater.Sci. Eng. A 244 (1998) 91.

[11] A.R. Boccaccini, C. Kaya, K.K. Chawla, Compos. Part A 32 (2001) 997.

[12] I. Zhitomorsky, J. Eur. Ceram. Soc. 18 (1998) 849.

[13] I. Zhitomirsky, L. Gal-Or, Mater. Lett. 38 (1999) 10.

[14] S. Shingubara, H. Kotani, H. Sakaue, F. Nishiyama, T. Takahagi, J.Vac. Sci. Technol. B 17 (6) (1999) 2553.

[15] D.T. Queheillat, D.D. Hass, D.J. Sypeck, H.N.G. Wadley, J. Mater. Res. Soc. 16 (2001) 1028.

[16] M. Amon, A. Bolz, M. Schaldach, J. Mater. Sci. Mater. Med. 7 (1996)

[17]Veprik, B. A., Kurylev, M.V., Korenkov, V. A., Mu- kazhanov, V. A. (1990): Composite SHS-powder of aluminum oxide with chrome for a plasma spraying, Abstracts Region. Conf. of Young Scientists and Experts of Research Organizations and Enterprises on Modern Materials in Mechanical Engineering, Perm, p. 14 [in Russian].

[18]Gorbatov, I. N., Shkiro, V. M., Terent ▪ ev, A.E., Shvedova, L.K., Martsenyuk, I. S., Karpenko, S.V. (1991): Study of properties of gas-thermal coatings from compositepowders of titanium and chromium carbides and nickel, Fizika i Khimiya Obrabotki Materialov, No 4, pp.102-106.

[19]Gorbatov, I. N., Il ▪ chenko, N. S., Terent ▪ ev, A. S. (1991): Effect of cladding double titanium-chrome carbide on the properties of plasma-sprayed coatings, Fizika i Khimiya Obrabotki Materialov, No 3, pp.69-73.